PHYSICAL REVIEW B **92**, 241404(R) (2015)

Valley-based Cooper pair splitting via topologically confined channels in bilayer graphene

Alexander Schroer,[1] Peter G. Silvestrov,[1] and Patrik Recher[1,2]
[1]*Institut für Mathematische Physik, Technische Universität Braunschweig, D-38106 Braunschweig, Germany*
[2]*Laboratory for Emerging Nanometrology Braunschweig, D-38106 Braunschweig, Germany*
(Received 22 September 2015; published 7 December 2015)

Bilayer graphene hosts valley-chiral one-dimensional modes at domain walls between regions of different interlayer potential or stacking order. When such a channel is close to a superconductor, the two electrons of a Cooper pair, which tunnel into it, move in opposite directions because they belong to different valleys related by the time-reversal symmetry. This kinetic variant of Cooper pair splitting requires neither Coulomb repulsion nor energy filtering but is enforced by the robustness of the valley isospin in the absence of atomic-scale defects. We derive an effective normal/superconducting/normal (NSN) model of the channel in proximity to an *s*-wave superconductor, calculate the conductance of split and spin-entangled pairs, and interpret it as a result of *local* Andreev reflection, in contrast to the widespread identification of Cooper pair splitting with crossed Andreev reflection in an NSN geometry.

DOI: 10.1103/PhysRevB.92.241404 PACS number(s): 72.80.Vp, 03.65.Ud, 74.45.+c

Creating mobile nonlocal spin-entangled electrons in a transport experiment with the help of superconductor–normal junctions has attracted a lot of attention in theory [1–8] and experiment [9–14] because the spin degree of freedom of the electron could serve as a solid-state qubit [15]. In the existing experiments, the envisaged process where a Cooper pair is split over two normal leads is crossed Andreev reflection (CAR) [16,17], which is enhanced by the repulsive electron-electron interaction on two quantum dots weakly coupled to the superconductor [1] or by energy filtering [2,18]. The basic mechanism of these entanglers is not very sensitive to the specific material used, i.e., the underlying band structure. It has been shown that characteristic features of new materials exhibiting Dirac cones like graphene or topological insulators can be useful for splitting Cooper pairs [7,19–24]. In these proposals, the efficiency of the splitting process, in the absence of interactions, relies on nonprotected resonance conditions or the split Cooper pair is not spin entangled due to spin helicity or spin polarization of the leads. Helical edge states of the quantum spin Hall regime have, however, been proposed to detect spin entanglement [8,25].

Here, we investigate a Cooper pair splitter based on local Andreev reflection (LAR). We propose to exploit the valley degree of freedom in bilayer graphene (BG), where valley-chiral, spin-degenerate one-dimensional (1D) channels are formed at domain walls. Such domain walls can be engineered by switching the sign of an interlayer voltage or by reversing the stacking order [26–28]. In proximity to a superconductor, Cooper pairs tunneling into the channel are split: two electrons propagate towards opposite terminals but remain spin entangled (Fig. 1), since, as required by time-reversal symmetry, the two electrons forming the Cooper pair in the superconductor are from different valleys [29]. In this scenario, normal reflection and CAR are absent for quasiparticles incoming from the normal part of the channel and scattering at the region with proximity-induced superconductivity. We find that generally, when normal transmission through the superconducting region is strong, nonlocal pair emission is equivalent to LAR, opposite to the case dominated by normal reflection, where CAR produces nonlocal pairs. Our BG implementation has unit splitting efficiency independent of

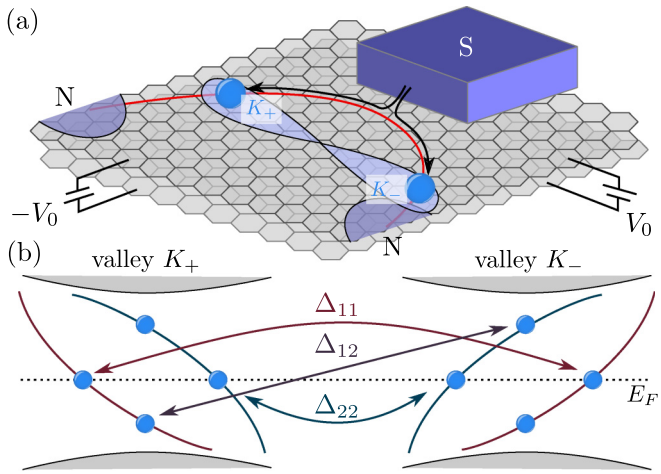

FIG. 1. (Color online) (a) At a domain wall (red) in BG between different interlayer voltages $\pm V_0$ or different stacking order a topological valley-chiral channel forms. Cooper pairs tunneling into it from a nearby *s*-wave superconductor (S) are split because the two electrons belong to opposite valleys $K_\pm$ and thus have opposite velocities. They remain spin entangled and propagate to separate normal leads (N). (b) In each valley two subgap modes along the domain wall emerge. Energy and momentum conservation along the NS interface fix four points in the spectrum where Cooper pairs are injected.

resonance conditions, provided the valley degree of freedom is robust. The device extends the upcoming "valleytronics" [30] to nonlocal Einstein-Podolsky-Rosen pairs. A 1D channel defined by opposite stacking order has recently been created experimentally in BG [31] with mean free paths over several hundreds of nanometers, demonstrating weak intervalley scattering.

We analyze the setup of Fig. 1 in two steps: first, we investigate the influence of the superconductor on the 1D channel by solving a Bogoliubov–de Gennes (BdG) equation, and derive an effective 1D model to describe the proximity effect in the channel. Second, we calculate the subgap conductance when applying a bias voltage between the superconductor and

the channel using a rate equation approach. We interpret the subgap transport in a scattering matrix picture and show that the outgoing scattered state is a two-particle spin-entangled state on top of a filled normal-state Fermi sea with a chemical potential lowered by the bias voltage. To leading order its weight is given by the LAR amplitude.

Model. We consider a BG sheet with Bernal AB stacking in the presence of an interlayer voltage $V(\boldsymbol{r})$ [32]. We model the superconductor region as BG in which the bands are shifted by a scalar potential $U(\boldsymbol{r})$ due to doping and which has an induced s-wave pairing amplitude $\Delta(\boldsymbol{r})$. We employ the low-energy approximation for BG, valid at energies and (inter)layer voltages smaller than the interlayer hopping $\gamma_1 \simeq 0.3$ eV. Without the superconductor, the valley index $\chi_v = \pm 1$ distinguishing the two K points $K_\pm = \pm(4\pi/3a, 0)$ and the electron spin $s = \pm 1 \equiv \uparrow, \downarrow$ are good quantum numbers and we write the Bogoliubov–de Gennes equation as $H_{\mathrm{BdG}}^{\chi_v,s}\Phi_{\chi_v,s}(\boldsymbol{r}) = \varepsilon\Phi_{\chi_v,s}(\boldsymbol{r})$,

$$H_{\mathrm{BdG}}^{\chi_v,s} = \{\alpha\hbar^2[2\chi_v\partial_x\partial_y\sigma_y + (\partial_x^2 - \partial_y^2)\sigma_x] + U(\boldsymbol{r}) + V(\boldsymbol{r})\sigma_z\}\tau_z + \Delta(\boldsymbol{r})\tau_x, \quad (1)$$

where $\alpha = v_F^2/\gamma_1$. The Pauli matrices σ_i act in the pseudospin (A_1, B_2) space and τ_i in electron-hole space and we set the Fermi energy $E_F = 0$. The four-component spinor is $\Phi_{\chi_v,s}(\mathbf{r}) = (\boldsymbol{u}_{\chi_v,s}(\boldsymbol{r}), \boldsymbol{v}_{\chi_v,s}(\boldsymbol{r}))^{\mathrm{T}}$ where we have introduced the electron $\boldsymbol{u}_{\chi_v,s}(\boldsymbol{r}) = (u_{A_1,\chi_v,s}(\boldsymbol{r}), u_{B_2,\chi_v,s}(\boldsymbol{r}))$ and hole components $(u \to v)$ on the two sublattices. Excitations with energy ε are then expanded as $\gamma_{\chi_v,s}(\varepsilon) = \int d^2r\, \Phi^*_{\chi_v,s}(\mathbf{r}) \cdot \Psi_{\chi_v,s}(\mathbf{r})$ with the vector of field operators $\Psi_{\chi_v,s}(\mathbf{r}) = (\psi_{A_1,\chi_v,s}(\boldsymbol{r}), \psi_{B_2,\chi_v,s}(\boldsymbol{r}), s\,\psi^\dagger_{A_1,-\chi_v,-s}(\boldsymbol{r}), s\,\psi^\dagger_{B_2,-\chi_v,-s}(\boldsymbol{r}))^{\mathrm{T}}$. We neglect skew-interlayer couplings, which induce trigonal warping at energies close above the gap [33] but do not break the (topological) subgap states [34].

In the absence of the superconductor $[\Delta(\boldsymbol{r}) = U(\boldsymbol{r}) = 0]$ and assuming the modes to propagate along the y direction along a domain wall at $x = 0$, i.e., $V(\boldsymbol{r}) = -V_0\,\mathrm{sgn}(x)$ with $V_0 > 0$, the topologically confined modes can be found analytically [26]. The electron and hole sectors in Eq. (1) decouple. In the electron sector, the solutions in each half space have the form $\Phi_{\chi_v,s}(\mathbf{r}) = (\boldsymbol{u}^0_{\chi_v,s}(\boldsymbol{r}), 0)^{\mathrm{T}}$ where $\boldsymbol{u}^0_{\chi_v,s}(\boldsymbol{r}) = \boldsymbol{u}^0_{\chi_v,s} e^{(i/\hbar)(p_x x + p_y y)}$ with

$$\boldsymbol{u}^0_{\chi_v,s} = \begin{pmatrix} -\varepsilon - V \\ \alpha^2(p_x + i\chi_v p_y)^2 \end{pmatrix}. \quad (2)$$

For any fixed energy ε and momentum p_y there are four allowed values $p_x = \pm\sqrt{\pm i\sqrt{V_0^2 - \varepsilon^2}/\alpha - p_y^2}$ which become complex when $|\varepsilon| < V_0$, i.e., there are no propagating modes in the bulk at energies below V_0. Matching the wave functions decaying away from the domain wall and their derivatives, one obtains the two electronic subgap solutions $n = 1,2$ in each valley, $\Phi^{0,n}_{\chi_v,s,p_y}(x)$, with the dispersion relation

$$\varepsilon^{0,1/2}_{\chi_v,s,p_y} = \pm\frac{\sqrt{2}V_0 - \alpha p_y^2}{2} - \frac{\chi_v p_y}{2}\sqrt{2\sqrt{2}\alpha V_0 + \alpha^2 p_y^2}, \quad (3)$$

with velocities opposite in the two valleys [26]. The solutions for the hole sector $\Phi^{0,3/4}_{\chi_v,s,p_y}(x) = (0, \boldsymbol{v}^0_{\chi_v,s}(\boldsymbol{r}))^{\mathrm{T}}$ where $\boldsymbol{v}^0_{\chi_v,s}(\boldsymbol{r})$ at energy $\varepsilon^{0,3/4}_{\chi_v,s,p_y}$ are obtained from Eqs. (2) and (3) by setting $\varepsilon \to -\varepsilon$.

The relevant momenta p_y are close to the K points: taking $\varepsilon \sim 0$, we obtain from Eq. (3) the momentum scale $p_y \sim \sqrt{V_0/\alpha}$, on which the K points are located at $\frac{4\pi\hbar}{3a}/\sqrt{V_0/\alpha} \sim 10^2$ for $V \sim \Delta \sim$ meV. The guided modes decay into the bulk on a length scale of $\sqrt{\hbar^2\alpha/V_0}$, which then is on the order of several tens of nanometers. This sets the scale of the separation between the guided mode and a superconductor required to obtain a proximity effect.

Perturbation theory for superconducting pairing. Assuming a superconductor/normal interface with translational invariance along the y direction, there are three distinct areas: in the superconductor area, $x < -d$, the pairing amplitude $\Delta(\boldsymbol{r}) = \Delta$ is finite and $U(\boldsymbol{r}) = -U_S$ is negative. The area $-d < x < 0$ is in the normal state as before, $\Delta = U_S = 0$, but the interlayer voltage is finite, $V = V_0 > 0$. This region is a tunnel barrier between the superconductor and the domain wall at the interface to the third region $x > 0$, where $\Delta = U_S = 0$ and $V = -V_0$. In this situation guided modes exist at $|\varepsilon| < \min(V_0, \Delta)$ because states above V_0 can propagate in the normal regions and states above Δ can propagate in the superconductor. Because of the tunnel barrier the guided modes are only weakly affected by the superconductor and we can apply standard quasidegenerate perturbation theory [35,36], for which the unperturbed Hamiltonian H_0 is obtained from H_{BdG} by setting $\Delta = U = 0$ everywhere and so the perturbation H_1, which adds the missing parts, is finite only at $x < -d$. As a result of the perturbation the electron and hole states of the channel acquire a finite overlap $\tilde{\Delta}_{nn'}(p_y)$, where n, n' label the subgap bands. This allows for particle number nonconserving processes, i.e., Cooper pair transport. To first order only the electron and hole states belonging to the same subgap band mix, $\tilde{\Delta}_{11} = \tilde{\Delta}_{22}$, $\tilde{\Delta}_{12} = 0$. This agrees with the result one expects when introducing superconductivity phenomenologically by constructing the BdG equation directly from the guided modes with a uniform pairing $\tilde{\Delta}_{11}\tau_x$. The second order corrections, which take into account the modification of the wave functions due to the superconductor, however, reveal that the situation is different in the geometry we consider. The electron hole overlap differs in both bands, $\tilde{\Delta}_{11} \neq \tilde{\Delta}_{22}$, and band mixing is finite, $\tilde{\Delta}_{12} \neq 0$ (Fig. 2) [37]. This is confirmed by the full dispersion relation of H_{BdG} we obtain by matching the four-component spinor and its derivatives at both interfaces numerically (Fig. 2, inset): two gaps of different size open at zero energy ($\tilde{\Delta}_{11}$ and $\tilde{\Delta}_{22}$) and two gaps open at zero momentum where electron and hole states from different subgap bands cross ($\tilde{\Delta}_{12} = \tilde{\Delta}^*_{21}$). This means that there is Cooper pair transport at zero energy as well as at the finite energies $\pm V_0/\sqrt{2}$.

Cooper pair transport. We use Fermi's golden rule to calculate the Cooper pair current $I = 2e\sum_{fi}(W^+_{fi} - W^-_{fi})\rho_i$, where $W^\pm_{fi} = \frac{2\pi}{\hbar}|\langle f_\pm \,|\, H_T \,|\, i\rangle|^2\delta(\varepsilon_f - \varepsilon_i)$ is the transition rate from an initial state i with probability ρ_i at energy ε_i to the final state $f_\pm$ with two more (less) electrons at energy ε_f. The tunnel Hamiltonian H_T comprises the particle number nonconserving terms of the second-quantized perturbative model with electron operators $c^n_{\chi_v,s}(k)$ and hole operators

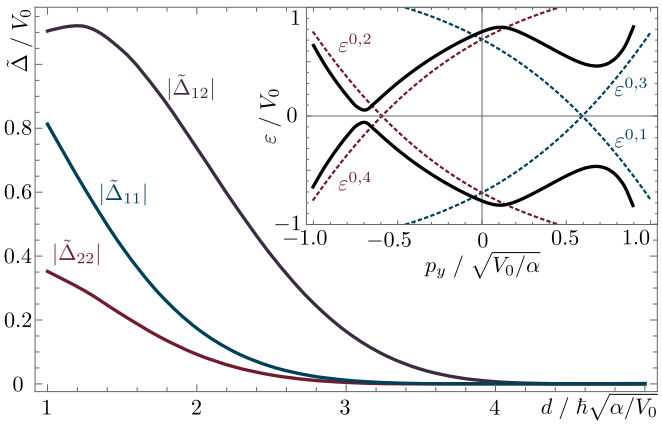

FIG. 2. (Color online) Induced intraband superconductivity $\tilde{\Delta}_{11}$ ($\tilde{\Delta}_{22}$) in the 1D channel at the respective Fermi point $p_y = \pm 2^{-3/4}\sqrt{V_0/\alpha}$ and induced interband superconductivity $\tilde{\Delta}_{12}$ at $p_y = 0$. For illustrative purposes we choose the bulk superconducting gap $\Delta = V_0$ and the doping $U_S = 10V_0$ ($\Delta < V_0$ is equally feasible). The amplitudes decay exponentially with the distance d to the superconductor because the $V > 0$ region acts as a tunnel barrier. Inset: In the normal state dispersion (dashed) two different-sized gaps open at the Fermi energy because $\tilde{\Delta}_{11} \neq \tilde{\Delta}_{22}$, shown for $d = 1.5\sqrt{\hbar^2\alpha/V_0}$. Additionally, $\tilde{\Delta}_{12}$ opens a gap at $p_y = 0$. This point contributes significantly to Cooper pair transport because compared to the Fermi points the normal density of states is higher and because the energy is larger so the bound states extend further into the bulk, increasing the coupling to the superconductor.

$h^n_{\chi_v,s}(k) \equiv s c^{n\dagger}_{-\chi_v,-s}(-k)$, where $k \equiv p_y$,

$$H_T = \sum_{\chi_v nn' ks} \tilde{\Delta}_{nn'}(k) s c^n_{\chi_v,s}(k) c^{n'}_{-\chi_v,-s}(-k) + \text{H.c.} \qquad (4)$$

Because the superconductor interface has a finite width w, we restrict the pairing amplitude in real space $\tilde{\Delta}(x,x')$ to $x,x' \in [-w/2, w/2]$. In momentum space (suppressing all indices) this amounts to $\sum_k \tilde{\Delta}(k) c_k c_{-k} \longrightarrow \sum_{kk'} \Delta_{kk'} c_k c_{k'}$ with $\tilde{\Delta}(k)$ from the microscopic calculation and

$$\Delta_{kk'} = \tilde{\Delta}\left(\frac{k-k'}{2}\right)\frac{L}{2\pi}\int dl \frac{\sin\left[(l-k)\frac{w}{2}\right]}{(l-k)\frac{L}{2}}\frac{\sin\left[(l+k')\frac{w}{2}\right]}{(l+k')\frac{L}{2}},$$

where L is the total length of the system, which does not enter the final results, and we have exploited that the integrand is peaked around $k \approx l \approx -k'$. With this, the rates for removing (adding) a Cooper pair, $|i\rangle \to |f\rangle = c^{n(\dagger)}_{\chi_v,s}(k) c^{n'(\dagger)}_{-\chi_v,-s}(k')|i\rangle$, become $W^{\mp}_{fi} = 4\pi|\Delta^{nn'}_{kk'}|^2 \langle \hat{n}^{n,e/h}_{\chi_v,s}(k)\rangle_i \langle \hat{n}^{n',e/h}_{-\chi_v,-s}(k')\rangle_i \delta[\varepsilon^n_{\chi_v}(k) + \varepsilon^{n'}_{-\chi_v}(k')]$, where at low temperatures the occupation probability $\langle \hat{n}^{n,e}_{\chi_v,s}(k)\rangle_i = 1 - \langle \hat{n}^{n,h}_{\chi_v,s}(k)\rangle_i \approx \Theta[-\delta\mu - \varepsilon^n_{\chi_v}(k)]$ with $\delta\mu$ the voltage applied between the superconductor and the channel. Rewriting the sum over momenta as energy integrals, the current becomes

$$I = \frac{32e}{\hbar}\frac{\pi L^2}{(2\pi)^2}\sum_{nn'}\int_{-\delta\mu}^{\delta\mu} d\varepsilon \left|\frac{\partial k_{K_+ n}(\varepsilon)}{\partial\varepsilon}\right|\left|\frac{\partial k_{K_- n'}(-\varepsilon)}{\partial\varepsilon}\right| \times |\Delta_{nn'}(\varepsilon, -\varepsilon)|^2. \qquad (5)$$

The combination of energy conservation and approximate momentum conservation implies that the pair tunneling probability $|\Delta_{nn'}(\varepsilon, -\varepsilon)|^2$ has a single peak as a function of ε for each pair n,n'. Injection into the same subgap band, $n = n'$, happens near $\varepsilon^{nn}_0 = 0$, and into different subbands, $n \neq n'$, near $\varepsilon^{12}_0 = -\varepsilon^{21}_0 = V_0/\sqrt{2}$ [Fig. 1(b)]. Linearizing the dispersion (3) around these points [36], $\varepsilon = \varepsilon^{nn'}_0 + \hbar v^{nn'}_0 (k - k^{nn'}_0)$, the tunnel amplitude becomes $\Delta_{nn'} = \tilde{\Delta}_{nn'}(k^{nn'}_0) \sin[(\varepsilon - \varepsilon^{nn'}_0)(w/\hbar v^{nn'}_0)]/L(\varepsilon - \varepsilon^{nn'}_0)$ and we obtain the conductance

$$G \approx 4G_0 \sum_{nn'} T_{nn'}\left[\delta_w\left(\delta\mu - \varepsilon^{nn'}_0\right) + \delta_w\left(\delta\mu + \varepsilon^{nn'}_0\right)\right], \qquad (6)$$

where $G_0 = 2e^2/h$ is the conductance quantum, $\delta_w(\varepsilon) = \hbar v^{nn'}_0 \sin^2[\varepsilon w/(\hbar v^{nn'}_0)]/(\pi w \varepsilon^2)$ becomes the delta function for $w \to \infty$, and $T_{nn'} = 2\pi w|\tilde{\Delta}(k^{nn'}_0)|^2/(\hbar v^{nn'}_0)$ is the effective tunneling strength. Note that the conductance grows with the length of the interface, in contrast to conventional Cooper pair splitters, which suffer from an exponential suppression in the spatial size. Here, Cooper pairs are split kinematically only after having tunneled locally into the channel, a process which can happen simultaneously along the whole interface. The conductance contains a central zero-bias peak and two characteristic side peaks [Fig. 3(a)], which arise because of the special subgap band structure and which correspond to the injection points marked in Fig. 1(b). The peak height is

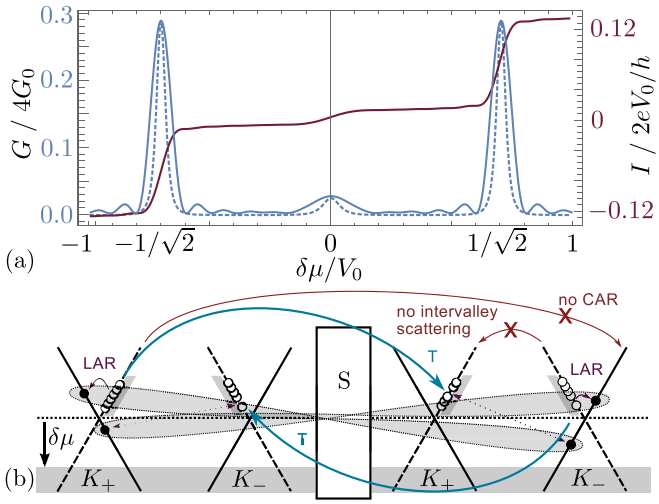

FIG. 3. (Color online) (a) Subgap conductance G and Cooper pair current I of a $w = 25\hbar\sqrt{\alpha/V_0}$ long interface between the superconductor and the 1D channel at a distance $d = 3\sqrt{\hbar^2\alpha/V_0}$ with $\Delta = U_S = V_0$. The peaks reflect simultaneous energy and approximate momentum conservation. The sharp boundary of the superconductor region causes oscillations which vanish if an exponential cutoff is used instead (dashed). (b) Scattering interpretation of Cooper pair splitting. Incoming holes (open circles) filled up to the bias $\delta\mu$ are transmitted (T) or undergo LAR. Reflection and CAR are zero by valley chirality. LAR creates an outgoing electron (filled circle) on the same side and no outgoing hole on the opposite side, i.e., an electron of opposite spin, momentum, and energy (dashed arrow), which are spin entangled (text).

proportional to the induced superconducting pairings. A factor of 4 arises due to the spin and valley degeneracy and a factor of 2 due to pair transport.

LAR and Cooper pair splitting. In Eq. (4) the singlet nature of the injected pairs is manifest. Cooper pair emission is closely related to Andreev reflection [38–40] and equivalent to CAR if the dominant scattering process is ordinary reflection. In our device, the 1D channel with a proximity-induced superconducting region is a NSN junction, in which, by chirality, only transmission through the S region with amplitude $t(\varepsilon)$ and *local* Andreev reflection (an incoming quasiparticle in valley $K_\pm$ is reflected as an outgoing antiparticle with opposite velocity in valley $K_\mp$) with amplitude $r(\varepsilon)$ are possible. We consider the general scattering problem with finite CAR and normal reflection in the Supplemental Material [36]. When a voltage bias $\delta\mu$ is applied between the superconductor and the channel to extract Cooper pairs, the incoming modes are filled with holes up to $E_F+\delta\mu$. Without the superconductor, all are transmitted and fill the outgoing modes up to $E_F+\delta\mu$, which is equivalent to a Fermi sea for electrons $|\rangle_{\delta\mu}$ with the Fermi energy $E_F-\delta\mu$ [39],

$$|\rangle_{\delta\mu} \equiv \prod_{\substack{0<\varepsilon<\delta\mu \\ \alpha s}} h_s^{\alpha\dagger}(\varepsilon)|\rangle \equiv \prod_{\substack{0<\varepsilon<\delta\mu \\ \alpha s}} c_s^{\alpha}(-\varepsilon)|\rangle. \tag{7}$$

Here, $|\rangle$ is the quasiparticle vacuum with respect to the Fermi level E_F of the superconductor and $h_s^{L/R\dagger}(\varepsilon)\equiv s c_{-s}^{L/R}(-\varepsilon)$ creates outgoing holes with spin s at energy $E_F+\varepsilon$ in the left/right lead, which is the same as annihilating an electron with opposite spin $-s$ at energy $E_F-\varepsilon$. We drop the valley index, which is fixed by the requirement that outgoing modes move away from the superconducting region, and the band index for simplicity [36]. Due to the proximity effect LAR becomes finite. The key observation is that when LAR occurs, no hole with spin s at energy $E_F+\varepsilon$ is transmitted to the other side. The outgoing mode is therefore occupied by a spin $-s$ electron at energy $E_F-\varepsilon$ [Fig. 3(b)]. To see this, we use Eq. (7) to write the outgoing state in terms of $|\rangle_{\delta\mu}$ [36],

$$\begin{aligned}\prod_{\substack{0<\varepsilon<\delta\mu \\ \alpha s}} &\left[s\,t\,c_{-s}^{\bar\alpha}(-\varepsilon)+r\,c_s^{\alpha\dagger}(\varepsilon)\right]c_{-s}^{\bar\alpha\dagger}(-\varepsilon)|\rangle_{\delta\mu} \\ &= \prod_{\substack{0<\varepsilon<\delta\mu \\ \alpha}} \{t^2+r^2 c_\uparrow^{\alpha\dagger}(\varepsilon)c_\downarrow^{\bar\alpha\dagger}(-\varepsilon)c_\downarrow^{\alpha\dagger}(\varepsilon)c_\uparrow^{\bar\alpha\dagger}(-\varepsilon) \\ &\quad + rt[c_\downarrow^{\alpha\dagger}(\varepsilon)c_\uparrow^{\bar\alpha\dagger}(-\varepsilon)-c_\uparrow^{\alpha\dagger}(\varepsilon)c_\downarrow^{\bar\alpha\dagger}(-\varepsilon)]\}|\rangle_{\delta\mu}. \end{aligned}\tag{8}$$

If r is small, it becomes $\{1+\sum_{\varepsilon\alpha} r[c_\downarrow^{\alpha\dagger}(\varepsilon)c_\uparrow^{\bar\alpha\dagger}(-\varepsilon)-c_\uparrow^{\alpha\dagger}(\varepsilon)c_\downarrow^{\bar\alpha\dagger}(-\varepsilon)]+O(r^2)\}|\rangle_{\delta\mu}$, where the desired nonlocal singlet state is explicit. Then, individual splitting events are separated and it is meaningful to talk about pairs. In this regime of interest the above perturbative result holds. Only the emitted pairs contribute to the shot noise of the scattering state. In the opposite limit of perfect LAR with $O(t)\sim 0$, $O(r)\sim 1$, the outgoing state is a nonentangled product state. LAR is most pronounced at $\varepsilon=0$ and $\varepsilon=\pm V_0/\sqrt{2}$ [Fig. 3(a)] where the superconductor opens gaps $\tilde\Delta_{nn'}$ in the spectrum for the case of an infinitely long ($w\to\infty$) tunnel junction (Fig. 2). LAR becomes weak for all energies, when w falls below the coherence lengths $\hbar v_0^{nn'}/\tilde\Delta_{nn'}$.

Conclusion. Our setup allows for highly efficient creation of nonlocal spin-entangled electrons without repulsive interaction or energy filters. The topological channel can be created in the bulk of the BG sample, completely avoiding sharp sample edges, the main source of intervalley scattering [41], which could reduce the splitting efficiency. Using an electrically tunable channel geometry, ballistic beam splitters could be created to prove the spin entanglement via noise [42], so far an elusive goal. Spin relaxation and decoherence in BG are expected to be weak due to the small spin-orbit coupling [43–45] and the sparsity of nuclear spins.

Acknowledgments. We thank A. Baumgartner, P. Samuelsson, C. Schönenberger, and A. Levy Yeyati for helpful discussions and acknowledge support from the EU-FP7 Project SE2ND, No. 271554, the DFG, Grant No. RE 2978/1-1 and Research Training Group GrK1952/1 "Metrology for Complex Nanosystems," and the Braunschweig International Graduate School of Metrology B-IGSM.

[1] P. Recher, E. V. Sukhorukov, and D. Loss, Phys. Rev. B **63**, 165314 (2001).
[2] G. Lesovik, T. Martin, and G. Blatter, Eur. Phys. J. B **24**, 287 (2001).
[3] P. Recher and D. Loss, Phys. Rev. B **65**, 165327 (2002).
[4] C. Bena, S. Vishveshwara, L. Balents, and M. P. A. Fisher, Phys. Rev. Lett. **89**, 037901 (2002).
[5] P. Recher and D. Loss, Phys. Rev. Lett. **91**, 267003 (2003).
[6] A. Levy Yeyati, F. S. Bergeret, A. Martin-Rodero, and T. M. Klapwijk, Nat. Phys. **3**, 455 (2007).
[7] J. Cayssol, Phys. Rev. Lett. **100**, 147001 (2008).
[8] K. Sato, D. Loss, and Y. Tserkovnyak, Phys. Rev. Lett. **105**, 226401 (2010).
[9] L. Hofstetter, S. Csonka, J. Nygård, and C. Schönenberger, Nature (London) **461**, 960 (2009).
[10] L. G. Herrmann, F. Portier, P. Roche, A. L. Yeyati, T. Kontos, and C. Strunk, Phys. Rev. Lett. **104**, 026801 (2010).
[11] J. Schindele, A. Baumgartner, and C. Schönenberger, Phys. Rev. Lett. **109**, 157002 (2012).
[12] A. Das, Y. Ronen, M. Heiblum, D. Mahalu, A. V. Kretinin, and H. Shtrikman, Nat. Commun. **3**, 1165 (2012).
[13] Z. B. Tan, D. Cox, T. Nieminen, P. Lähteenmäki, D. Golubev, G. B. Lesovik, and P. J. Hakonen, Phys. Rev. Lett. **114**, 096602 (2015).
[14] R. S. Deacon, A. Oiwa, J. Sailer, S. Baba, Y. Kanai, K. Shibata, K. Hirakawa, and S. Tarucha, Nat. Commun. **6**, 7446 (2015).
[15] D. Loss and D. P. DiVincenzo, Phys. Rev. A **57**, 120 (1998).

[16] J. Torrès and T. Martin, Eur. Phys. J. B **12**, 319 (1999).
[17] G. Falci, D. Feinberg, and F. W. J. Hekking, Europhys. Lett. **54**, 255 (2001).
[18] I. A. Sadovskyy, G. B. Lesovik, and V. M. Vinokur, New J. Phys. **17**, 103016 (2015).
[19] C. Benjamin and J. K. Pachos, Phys. Rev. B **78**, 235403 (2008).
[20] J. Linder, M. Zareyan, and A. Sudbø, Phys. Rev. B **80**, 014513 (2009).
[21] W. Chen, R. Shen, L. Sheng, B. G. Wang, and D. Y. Xing, Phys. Rev. B **84**, 115420 (2011).
[22] R. W. Reinthaler, P. Recher, and E. M. Hankiewicz, Phys. Rev. Lett. **110**, 226802 (2013).
[23] J. Nilsson, A. R. Akhmerov, and C. W. J. Beenakker, Phys. Rev. Lett. **101**, 120403 (2008).
[24] J. Wang, L. Hao, and K. S. Chan, Phys. Rev. B **91**, 085415 (2015).
[25] W. Chen, R. Shen, L. Sheng, B. G. Wang, and D. Y. Xing, Phys. Rev. Lett. **109**, 036802 (2012).
[26] I. Martin, Y. M. Blanter, and A. F. Morpurgo, Phys. Rev. Lett. **100**, 036804 (2008).
[27] A. Vaezi, Y. Liang, D. H. Ngai, L. Yang, and E.-A. Kim, Phys. Rev. X **3**, 021018 (2013).
[28] F. Zhang, A. H. MacDonald, and E. J. Mele, Proc. Natl. Acad. Sci. USA **110**, 10546 (2013).
[29] C. W. J. Beenakker, Rev. Mod. Phys. **80**, 1337 (2008).
[30] A. Rycerz, J. Tworzydlo, and C. W. J. Beenakker, Nat. Phys. **3**, 172 (2007).
[31] L. Ju, Z. Shi, N. Nair, Y. Lv, C. Jin, J. Velasco, Jr., C. Ojeda-Aristizabal, H. A. Bechtel, M. C. Martin, A. Zettl, J. Analytis, and F. Wang, Nature (London) **520**, 650 (2015).
[32] E. McCann and V. I. Fal'ko, Phys. Rev. Lett. **96**, 086805 (2006).
[33] E. McCann and M. Koshino, Rep. Prog. Phys. **76**, 056503 (2013).
[34] The subgap dispersion is, however, affected by trigonal warping [46]. This is negligible and our results hold quantitatively if $|V(\mathbf{r})| \gg \varepsilon_L$ in the bulk, where ε_L is the Lifshitz energy [33] .
[35] R. Winkler, *Spin-Orbit Coupling Effects in Two-Dimensional Electron and Hole Systems* (Springer-Verlag, Berlin, 2003).
[36] See Supplemental Material at http://link.aps.org/supplemental/10.1103/PhysRevB.92.241404 for further details.
[37] See F. Parhizgar and A. M. Black-Schaffer, Phys. Rev. B **90**, 184517 (2014) for a similar effect in bilayer systems with different superconductivity in each layer. .
[38] E. Prada and F. Sols, Eur. Phys. J. B **40**, 379 (2004).
[39] P. Samuelsson, E. V. Sukhorukov, and M. Büttiker, New J. Phys. **7**, 176 (2005).
[40] P. Samuelsson, E. V. Sukhorukov, and M. Büttiker, Phys. Rev. Lett. **91**, 157002 (2003).
[41] S. Das Sarma, S. Adam, E. H. Hwang, and E. Rossi, Rev. Mod. Phys. **83**, 407 (2011).
[42] G. Burkard, D. Loss, and E. V. Sukhorukov, Phys. Rev. B **61**, R16303(R) (2000).
[43] R. van Gelderen and C. M. Smith, Phys. Rev. B **81**, 125435 (2010).
[44] F. Guinea, New J. Phys. **12**, 083063 (2010).
[45] S. Konschuh, M. Gmitra, D. Kochan, and J. Fabian, Phys. Rev. B **85**, 115423 (2012).
[46] A. S. Núñez, E. Suárez Morell, and P. Vargas, Appl. Phys. Lett. **98**, 262107 (2011).